AAC Journals.ASM.org

High-Content Screening Technology Combined with a Human Granuloma Model as a New Approach To Evaluate the Activities of Drugs against *Mycobacterium tuberculosis*

Mayra Silva-Miranda,[a] Euloge Ekaza,[a] Adrien Breiman,[a] Karim Asehnoune,[b,c] David Barros-Aguirre,[d] Kevin Pethe,[e] Fanny Ewann,[e] Priscille Brodin,[e,f] Lluís Ballell-Pages,[d] Frédéric Altare[a]

INSERM–U892, CNRS UMR 6299, Université de Nantes, Nantes, France[a]; Laboratoire UPRES EA3826, Thérapeutiques Cliniques et Expérimentales des Infections, Faculté de Médecine, Université de Nantes, Nantes, France[b]; CHU Nantes, Pôle Anesthésie Réanimations, Service d'Anesthésie Réanimation Chirurgicale, Hôtel Dieu, Nantes, France[c]; Diseases of the Developing World, GlaxoSmithKline, Tres Cantos, Madrid, Spain[d]; INSERM Avenir, Institut Pasteur Korea, Bundang-gu, Seongnam-si, Gyeonggi-do, South Korea[e]; INSERM–U1019, CNRS UMR8204, Université de Lille, Nord de France, Institut Pasteur de Lille, Center for Infection and Immunity, Lille, France[f]

Tuberculosis remains a major health problem due to the emergence of drug-resistant strains of *Mycobacterium tuberculosis*. Some models have provided valuable information about drug resistance and efficacy; however, the translation of these results into effective human treatments has mostly proven unsuccessful. In this study, we adapted high-content screening (HCS) technology to investigate the activities of antitubercular compounds in the context of an *in vitro* granuloma model. We observed significant shifts in the MIC_{50}s between the activities of the compounds under extracellular and granuloma conditions.

Tuberculosis (TB) is a respiratory disease that is one of the major causes of mortality and morbidity worldwide. Almost 20 people develop TB and four patients die from the disease every minute somewhere in the world (1). The disease can be cured by drug treatment involving a regimen of several drugs. The World Health Organization (WHO) estimates that there were around 0.5 million new cases of multidrug-resistant TB (MDR-TB) in 2012 (2, 3). A recent report confirmed that MDR-TB is a continuing worldwide health problem, even in high-income countries with a low incidence of TB (4).

The immune system undoubtedly plays a major role in TB control (5). Signaling events of the immune system lead to the formation of a granuloma, the hallmark of TB. Granulomas are an immune microenvironment in which the infection can be controlled but also a niche in which bacilli can thrive and modulate immune responses to ensure their survival for long periods without causing damage (6, 7). Granulomas are cell aggregates that form tridimensional and heterogeneous structures (8, 9). We previously described an *in vitro* granuloma model involving human blood cells either infected with mycobacteria or incubated with mycobacterial antigens (8, 10). Either of these models resulted in the formation of a typical epithelioid granuloma with morphological characteristics and properties of cellular differentiation similar to those of natural granulomas (8, 10, 11). This model may help bridge the gap between the *in vitro* evaluation of MICs and costly *in vivo* efficacy studies in guinea pigs. In particular, compounds that are effective in the *in vitro* granuloma model could be prioritized for guinea pig studies.

High-content screening (HCS) technology has been used to identify anti-TB compounds (12–14). This technology has several advantages over traditional phenotypic screening approaches. This technology has mostly been used in single-cell experiments, because it is adapted to identify and analyze images (12, 13); however, in this paper, we focus on the use of granulomas instead of single cells. In this report, we describe the development of a novel HCS method to evaluate the activities of reference compounds against a green fluorescent protein (GFP)-expressing H37Rv strain of *Mycobacterium tuberculosis* (MTB-GFP) within 5 days, and we compared the MIC_{50} values with those of classical liquid cultures (extracellular), intracellular growth (single-cell assay), and within granulomas, all using the same bacterial strain.

MTB-GFP strains (13) were grown for 3 weeks at 37°C until the log phase was reached. The test inoculum was prepared by diluting the culture with phosphate-buffered saline (PBS) medium or complete RPMI (RPMIc) medium (containing RPMI 1640 medium supplemented with 10% heat-inactivated fetal bovine serum [FBS], with 1% glutamine, 1% HEPES, 1% nonessential amino acids) to a final bacterial concentration of 1×10^6 CFU/ml.

In vitro human granuloma formation was performed by incubating peripheral blood mononuclear cells (PBMC) of healthy volunteers; the cells were purified by gradient density sedimentation (15) with MTB-GFP using an appropriate multiplicity of infection in RPMIc medium at 37°C with low shaking (125 rpm) for 1 h; they were then washed with PBS containing 2% FBS and suspended in RPMIc medium at a concentration of 3.5×10^5 cells per well in 384-well plates (Greiner). The cells were then incubated for 3 days at 37°C in a 5% CO_2 atmosphere to allow the formation of granulomas.

Intragranuloma bacterial quantification was performed by fixing granulomas with 4% paraformaldehyde (Electron Microscopy Sciences) in PBS and staining with Hoechst (Sigma); each step consisted of a 30-min incubation period at room temperature.

Received 23 June 2014 **Returned for modification** 1 August 2014
Accepted 18 October 2014

Accepted manuscript posted online 27 October 2014

Citation Silva-Miranda M, Ekaza E, Breiman A, Asehnoune K, Barros-Aguirre D, Pethe K, Ewann F, Brodin P, Ballell-Pages L, Altare F. 2015. High-content screening technology combined with a human granuloma model as a new approach to evaluate the activities of drugs against *Mycobacterium tuberculosis*. Antimicrob Agents Chemother 59:693–697. doi:10.1128/AAC.03705-14.

Address correspondence to Frédéric Altare, frederic.altare@inserm.fr.

M.S.-M. and E.E. contributed equally to this work.

doi:10.1128/AAC.03705-14

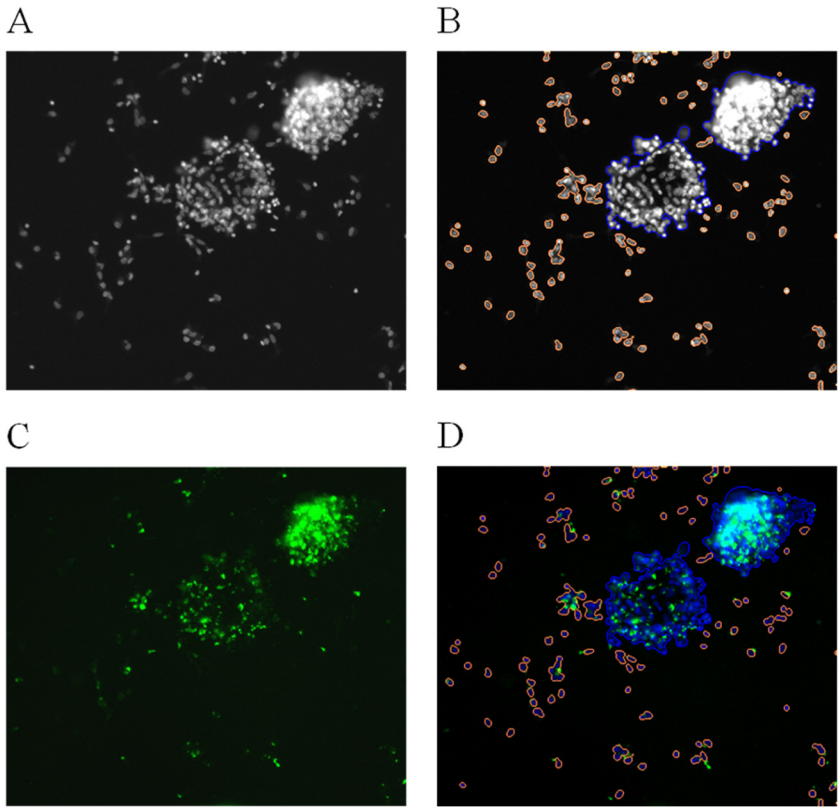

FIG 1 Typical granuloma images recorded by the automated CellInsight Thermo ArrayScan. Shown are the same image at 10× objective in one field (A), in the blue channel, with selected granulomas in blue and isolated cells or aggregated cells in orange (B), in the green channel, with bacteria as green spots (C), and as a composite image of the two channels (D).

The plates were sealed with optical adhesive film (Excel Scientific), and the images were recorded using CellInsight Thermo ArrayScan HCS equipment (Thermo Fisher Scientific) with a 10× objective. A 386-nm laser with an exposure time of 4 ms was used to analyze Hoechst staining, and a 485-nm laser with an exposure time of 597.286 ms was used to analyze GFP fluorescence. Each image was processed using Cellomics ArrayScan compartmental analysis (version 3). For the acquisition of the entire 384-well microtiter plate, 16 fields within each well were recorded. All fields contained two images, cell nuclei (blue channel) and bacteria (green channel). The granuloma structures were selected according to nuclei staining, due to the complexity of the size and form of the cells. Tests were carried out to evaluate the different settings used to identify granulomas, and the blue channel was finally chosen for identifying the granulomas (Fig. 1B). Using this approach, the granulomas could easily be distinguished from the PBMC and single cells, and cell aggregates could be eliminated. Spot detection was used to detect bacteria, because this approach can detect a single bacterium and thus give the exact number of bacteria (Fig. 1C). This method was validated in experiments involving suspensions of bacteria of known concentrations. Some variables generated from the granuloma protocol are the number of granulomas, area, size, intensity, spot, and number of granulomas/spot.

A dose-response assay to determine the MICs was performed by testing four drugs: isoniazid (INH), moxifloxacin (MOX), linezolid (LZD), and pyrazinamide (PZA). We used INH as a reference control because it is a potent mycobactericidal drug and a vital component of current combination regimens. LZD was chosen as an example of a compound that has recently shown great promise in the clinical setting, despite poor performance in murine animal models of TB (16). PZA has poor *in vitro* anti-TB activity when used alone but can boost other anti-TB drugs when used in combination, both in animal models and in the clinic setting. MOX is a promising potential candidate for future drug regimens, given its advanced clinical development status. We did not observe any toxic effects to cells with the concentrations of drugs tested. Stock solutions were prepared in high-grade dimethyl sulfoxide (DMSO) (Sigma) at a concentration of 200 mM and diluted for the assay with RPMIc to an appropriate concentration. The granulomas were exposed to compounds for 5 days under the same conditions as those previously described in order to evaluate their effect on MTB-GFP-colonized granulomas. After exposure, intragranuloma bacterial quantification was done as previously described. All experimental settings were kept constant to ensure that the same parameters were used in all analyses. However, all settings were recalibrated with respect to the granuloma control image for each sample. The ArrayScan Cellomics software provides many experimental variables; however, we focused on the number of granulomas, the total spot count (number of bacteria), and the number of spots per granuloma (*M. tuberculosis* cells per granuloma). The control granulomas and drug-treated granulomas were compared to evaluate whether the drug brought about a reduction in the number of bacteria in the granuloma (MTB/granuloma). The number of spots and the number of gran-

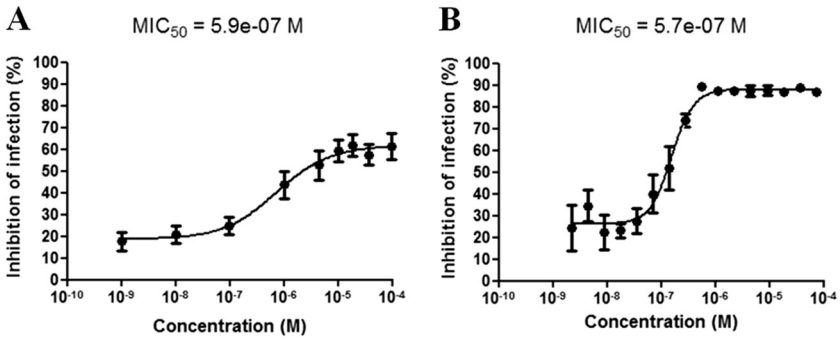

FIG 2 Comparison of the effect of the reference drug isoniazid against MTB-GFP in our *in vitro* granuloma assay (A) and its effect in murine Raw 264.7 macrophage assays (B). These two assays yielded similar dose-response curves. The results (mean ± standard deviation [SD] correspond to 9 independent donors for panel A and 4 independent experiments for panel B) were normalized according to DMSO and INH control values.

ulomas were used as internal controls. The effect of the drug was calculated as the percentage of inhibition of infection (PII), as follows: PII = $[1 - (\text{sample}_{\text{MTB/granuloma}}/\text{DMSO}_{\text{MTB/granuloma}})] \times 100$. The experiment was repeated six times for each concentration for each donor. The intragranuloma MIC_{50} was defined as the concentration of drug required to achieve a 50% inhibition of bacillus growth after 5 days of drug exposure. The MIC_{50} was determined from the dose-response curves. The data analysis was carried out with the GraphPad Prism version 5.02 software.

In the assay, DMSO did not show any toxic effect for cells at its highest concentration (0.05% [vol/vol]). The number of granulomas was used in our assay as an internal control for compound toxicity. We verified the lack of toxicity of DMSO at a concentration of 0.05% in granulomas by comparing the number of granulomas obtained in the presence of DMSO and that obtained with control samples (without the addition of any compound); no differences were found in the number of granulomas. Reference compounds, such as INH, containing the same DMSO concentration were evaluated in parallel. We found that the number of MTB-GFP inside the granulomas was unchanged after 5 days of incubation of infected cells with any compound (as a control) or with DMSO. The reduction in the number of MTB-GFP inside the granulomas treated with INH was thus due only to the effect of the drug and not to any toxic effect of the DMSO contained in the drug sample added to the cells (data not shown).

The GFP-based readout reflects the number of viable bacteria in the sample after antibiotic treatment. We used INH as a reference drug against MTB-GFP as previously described for a single-cell assay (12, 13). Dose-response curves were calculated with concentrations ranging from 1×10^{-9} M to 1×10^{-4} M, which were the same as those used for a previously reported single-cell assay (12). We calculated the PII of various concentrations of INH plotted as an INH dose-response curve (Fig. 2). Each point represents the PBMC isolated from at least nine healthy donors, and the standard deviation is shown. At a concentration of 10^{-9} M, the PII was 18% and was directly proportional to the INH concentration until reaching a plateau of 60% at 10^{-5} M. Thus, the MIC_{50} under these experimental conditions was around 0.59×10^{-6} or 0.59 μM (i.e., 0.081 μg/ml) (Fig. 2A). This value is similar to that calculated for INH in the single-cell assay, with an MIC_{50} of 0.57 μM (i.e., 0.078 μg/ml) (Fig. 2B). In addition, the single-cell assay results have been demonstrated to show a good correlation between the fluorescence counts and CFU counts obtained for reference compounds (12, 13). However, HCS screening would never replace the CFU determination method, which is currently the only technique that enables the exact determination of intracellular bacterial load, even though it gives a faster determination of the ability of a given drug to kill bacteria and enables a faster determination of the MIC of a drug.

The antimycobacterial activities of various compounds against MTB-GFP were determined by calculating the PII for each experimental concentration (ranging from 1 nM to 1 mM) to assess the sensitivities of the bacteria inside artificial granulomas. At low compound concentrations, the mean of the PII was low as a result of MTB-GFP replication (high number of bacilli in granulomas). At higher concentrations, the mean of the PII increased, due to the diminished number of bacilli in the granulomas. An inhibition of infection of 100% was not reached with any drug (Fig. 3). We calculated the MIC_{50}s of drugs from dose-response curves and compared them to those of extracellular and intracellular (in isolated macrophage cultures) bacterial growth assays, performed in parallel. The extracellular and intracellular MIC_{50} values were obtained as previously described by Remuiñán et al. (17) and Christophe et al. (13), respectively. Under normal assay conditions (medium pH ~7), the MIC_{50}s of INH, MOX, LZD, and PZA against intracellular (artificial granuloma) MTB-GFP were 0.081, 4.12, 1.65, and >5 μg/ml, respectively (Fig. 3). The MIC_{50}s of INH, MOX, LZD, and PZA against extracellular MTB-GFP were 0.05, 0.33, 0.098, and >5 μg/ml, respectively. The MIC_{50}s of INH, MOX, LZD, and PZA to intracellular bacteria (in macrophages) were 0.052, 0.27, 0.159, and >5 μg/ml, respectively. A modest but still measurable activity of PZA under the artificial granuloma conditions was observed. Previous reports found that PZA is devoid of any significant anti-TB activity under extracellular growth conditions at concentrations up to 2 mg/ml (18), although some activity is observed when bacteria are grown at pH 5.5, with an MIC_{50} between 62.5 and 125 μg/ml (19). Reports of the activity of PZA in infected macrophages are conflicting; some studies found that PZA was completely inactive (20, 21), whereas another report found that PZA had a modest effect at around 20 μg/ml (22). For MOX and LZD, our results showed a shift (10- to 15-fold) in the MIC_{50}s between the activities of the compounds under extracellular and artificial granuloma conditions. The MTB-GFP resistance in an artificial granuloma model can be explained by the poor permeability associated with the complex cellular composition of the granuloma, which may prevent the compound from

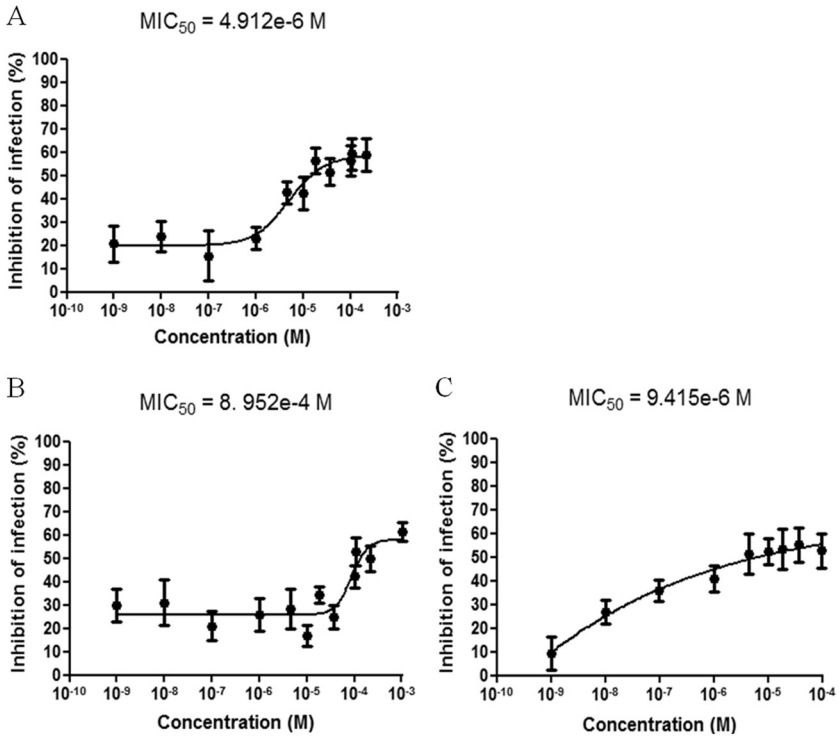

FIG 3 Dose-response curves for various anti-TB agents in artificial granuloma assay. The antimycobacterial effect of each agent was determined by calculating the percentage of inhibition of infection. We obtained MIC_{50}s of 1.65 μg/ml for LZD (A), 101.2 μg/ml for PZA (B), and 4.12 μg/ml for MOX(C).

reaching the mycobacteria (8, 9). In addition, it has been well-known for decades that inside the granuloma, the bacteria change their physiological characteristics (11) and especially their external envelope; therefore, their susceptibility to a given drug may be completely different from that under extracellular conditions or even within single cells. Indeed, without the lymphocyte environment present around infected macrophages within the granulomas, the macrophage intracellular environment is different in single-cell assays, and a different environment with the bacterial physiology may obviously trigger different types of physiological adaptation by the bacteria and thus a different susceptibility to the same drug. These differences in the bacterial physiological state and thus its variable drug susceptibility is one of the main reasons why we found it very important to develop a model of granuloma to evaluate the bacterial susceptibilities to given drugs, because it would of course be far more relevant to the natural environment of the bacilli within infected individuals, where they are located in granulomas. Altogether, these factors represent many obstacles for compounds to access bacteria and may thus render them less susceptible to small-molecule inhibitors, as was previously encountered in assays with nonreplicating bacteria. In both instances, this seems to indicate that our *in vitro* granuloma model shows a close resemblance to the low clearance rate of bacteria observed in the clinic setting. Indeed, in this setting, systemic exposure to high concentrations of anti-TB agents is generally required for prolonged periods to generate only small CFU reductions in the lungs of infected patients during the prolonged phase of anti-TB treatment (23, 24).

The main advantage of this technology is that the MIC can quickly be determined for compounds effective against intracellular bacilli, and these values show a good correlation with the CFU counts obtained for reference compounds (12). We adapted HCS to screen reference compounds that target mycobacteria inside artificial granulomas. We used FBS in our assay to avoid interference with human immune factors, except for those produced by PBMC. Additionally, we removed the extracellular nonphagocytosed bacilli by selecting only mature granulomas of index 2 to 4, as described previously (25). This ensured that only internalized bacteria were counted, such that the assay specifically measured the effects of compounds on mycobacteria inside the granuloma. The significant shifts in the MICs observed between the activities of the compounds under extracellular and artificial granuloma conditions highlight the important differences between traditional methods to assess MICs and the artificial *in vitro* granuloma system. The assessment of MICs in granulomas is consistent with the clinical reality that high concentrations of antibiotic administered over long periods of time are required to generate significant reductions in the CFU burdens of infected patients.

ACKNOWLEDGMENTS

Financial support for this work was provided by the European Community toward the Open Collaborative Model for Tuberculosis Lead Optimization (ORCHID) (grant agreement 261378), ERC-STG grant 260901, MM4TB grant 260872, the Korea Research Foundation grant K20802001409-09B1300-03700, and INSERM-Avenir.

We thank Lourdes Encinas for the quick and efficient transfer of compounds between the different labs involved in this work, Pascale Bemer and her team for biosafety level 3 (BSL3) laboratory access, and Vincent Delorme for data analysis.

REFERENCES

1. **Kaufmann SH.** 2011. Fact and fiction in tuberculosis vaccine research: 10 years later. Lancet Infect Dis **11:**633–640. http://dx.doi.org/10.1016/S1473-3099(11)70146-3.
2. **World Health Organization.** 2013. Global tuberculosis report 2013. WHO/HTM/TB/2013.11. World Health Organization, Geneva, Switzerland. http://apps.who.int/iris/bitstream/10665/91355/1/9789241564656_eng.pdf.
3. **Zignol M, Hosseini MS, Wright A, Weezenbeek CL, Nunn P, Watt CJ, Williams BG, Dye C.** 2006. Global incidence of multidrug-resistant tuberculosis. J Infect Dis **194:**479–485. http://dx.doi.org/10.1086/505877.
4. **Sotgiu G, D'Ambrosio L, Centis R, Bothamley G, Cirillo DM, De Lorenzo S, Guenther G, Kliiman K, Muetterlein R, Spinu V, Villar M, Zellweger JP, Sandgren A, Huitric E, Lange C, Manissero D, Migliori GB.** 2012. Availability of anti-tuberculosis drugs in Europe. Eur Respir J **40:**500–503. http://dx.doi.org/10.1183/09031936.00009212.
5. **Getahun H, Gunneberg C, Granich R, Nunn P.** 2010. HIV infection-associated tuberculosis: the epidemiology and the response. Clin Infect Dis **50**(Suppl 3)**:**S201–S207. http://dx.doi.org/10.1086/651492.
6. **Adams DO.** 1976. The granulomatous inflammatory response. A review. Am J Pathol **84:**164–192.
7. **Sandor M, Weinstock JV, Wynn TA.** 2003. Granulomas in schistosome and mycobacterial infections: a model of local immune responses. Trends Immunol **24:**44–52. http://dx.doi.org/10.1016/S1471-4906(02)00006-6.
8. **Puissegur MP, Botanch C, Duteyrat JL, Delsol G, Caratero C, Altare F.** 2004. An *in vitro* dual model of mycobacterial granulomas to investigate the molecular interactions between mycobacteria and human host cells. Cell Microbiol **6:**423–433. http://dx.doi.org/10.1111/j.1462-5822.2004.00371.x.
9. **Gonzalez-Juarrero M, Turner OC, Turner J, Marietta P, Brooks JV, Orme IM.** 2001. Temporal and spatial arrangement of lymphocytes within lung granulomas induced by aerosol infection with *Mycobacterium tuberculosis*. Infect Immun **69:**1722–1728. http://dx.doi.org/10.1128/IAI.69.3.1722-1728.2001.
10. **Lay G, Poquet Y, Salek-Peyron P, Puissegur MP, Botanch C, Bon H, Levillain F, Duteyrat JL, Emile JF, Altare F.** 2007. Langhans giant cells from *M. tuberculosis*-induced human granulomas cannot mediate mycobacterial uptake. J Pathol **211:**76–85. http://dx.doi.org/10.1002/path.2092.
11. **Russell DG, Cardona PJ, Kim MJ, Allain S, Altare F.** 2009. Foamy macrophages and the progression of the human tuberculosis granuloma. Nat Immunol **10:**943–948. http://dx.doi.org/10.1038/ni.1781.
12. **Christophe T, Jackson M, Jeon HK, Fenistein D, Contreras-Dominguez M, Kim J, Genovesio A, Carralot JP, Ewann F, Kim EH, Lee SY, Kang S, Seo MJ, Park EJ, Škovierová H, Pham H, Riccardi G, Nam JY, Marsollier L, Kempf M, Joly-Guillou ML, Oh T, Shin WK, No Z, Nehrbass U, Brosch R, Cole ST, Brodin P.** 2009. High content screening identifies decaprenyl-phosphoribose 2′ epimerase as a target for intracellular antimycobacterial inhibitors. PLoS Pathog **5:**e1000645. http://dx.doi.org/10.1371/journal.ppat.1000645.
13. **Christophe T, Ewann F, Jeon HK, Cechetto J, Brodin P.** 2010. High-content imaging of *Mycobacterium tuberculosis*-infected macrophages: an *in vitro* model for tuberculosis drug discovery. Future Med Chem **2:**1283–1293. http://dx.doi.org/10.4155/fmc.10.223.
14. **Pethe K, Bifani P, Jang J, Kang S, Park S, Ahn S, Jiricek J, Jung J, Jeon HK, Cechetto J, Christophe T, Lee H, Kempf M, Jackson M, Lenaerts AJ, Pham H, Jones V, Seo MJ, Kim YM, Seo M, Seo JJ, Park D, Ko Y, Choi I, Kim R, Kim SY, Lim S, Yim SA, Nam J, Kang H, Kwon H, Oh CT, Cho Y, Jang Y, Kim J, Chua A, Tan BH, Nanjundappa MB, Rao SP, Barnes WS, Wintjens R, Walker JR, Alonso S, Lee S, Kim J, Oh S, Oh T, Nehrbass U, Han SJ, No Z, Lee J, Brodin P, Cho SN, Nam K, Kim J.** 2013. Discovery of Q203, a potent clinical candidate for the treatment of tuberculosis. Nat Med **19:**1157–1160. http://dx.doi.org/10.1038/nm.3262.
15. **Altare F, Durandy A, Lammas D, Emile JF, Lamhamedi S, Le Deist F, Drysdale P, Jouanguy E, Döffinger R, Bernaudin F, Jeppsson O, Gollob JA, Meinl E, Segal AW, Fischer A, Kumararatne D, Casanova JL.** 1998. Impairment of mycobacterial immunity in human interleukin-12 receptor deficiency. Science **280:**1432–1435. http://dx.doi.org/10.1126/science.280.5368.1432.
16. **Lee M, Lee J, Carroll MW, Choi H, Min S, Song T, Via LE, Goldfeder LC, Kang E, Jin B, Park H, Kwak H, Kim H, Jeon HS, Jeong I, Joh JS, Chen RY, Olivier KN, Shaw PA, Follmann D, Song SD, Lee JK, Lee D, Kim CT, Dartois V, Park SK, Cho SN, Barry CE, III.** 2012. Linezolid for treatment of chronic extensively drug-resistant tuberculosis. N Engl J Med **367:**1508–1518. http://dx.doi.org/10.1056/NEJMoa1201964.
17. **Remuiñán MJ, Pérez-Herrán E, Rullás J, Alemparte C, Martínez-Hoyos M, Dow DJ, Afari J, Mehta N, Esquivias J, Jiménez E, Ortega-Muro F, Fraile-Gabaldón MT, Spivey VL, Loman NJ, Pallen MJ, Constantinidou C, Minick DJ, Cacho M, Rebollo-López MJ, González C, Sousa V, Angulo-Barturen I, Mendoza-Losana A, Barros D, Besra GS, Ballell L, Cammack N.** 2013. Tetrahydropyrazolo[1,5-*a*]pyrimidine-3-carboxamide and *N*-benzyl-6′,7′-dihydrospiro[piperidine-4,4′-thieno[3,2-*c*]pyran] analogues with bactericidal efficacy against *Mycobacterium tuberculosis* targeting MmpL3. PLoS One **8:**e60933. http://dx.doi.org/10.1371/journal.pone.0060933.
18. **Zhang Y, Mitchison D.** 2003. The curious characteristics of pyrazinamide: a review. Int J Tuberc Lung Dis **7:**6–21.
19. **Heifets LB, Lindholm-Levy PJ.** 1990. Is pyrazinamide bactericidal against *Mycobacterium tuberculosis*? Am Rev Respir Dis **141:**250–252. http://dx.doi.org/10.1164/ajrccm/141.1.250.
20. **Rastogi N, Potar MC, David HL.** 1988. Pyrazinamide is not effective against intracellularly growing *Mycobacterium tuberculosis*. Antimicrob Agents Chemother **32:**287. http://dx.doi.org/10.1128/AAC.32.2.287.
21. **Heifets L, Higgins M, Simon B.** 2000. Pyrazinamide is not active against *Mycobacterium tuberculosis* residing in cultured humanmonocyte-derived macrophages. Int J Tuberc Lung Dis **4:**491–495.
22. **Crowle AJ, Sbarbaro JA, May MH.** 1986. Inhibition by pyrazinamide of tubercle bacilli within cultured human macrophages. Am Rev Respir Dis **134:**1052–1055.
23. **Diacon AH, Dawson R, von Groote-Bidlingmaier F, Symons G, Venter A, Donald PR, van Niekerk C, Everitt D, Winter H, Becker P, Mendel CM, Spigelman MK.** 2012. 14-day bactericidal activity of PA-824, bedaquiline, pyrazinamide, and moxifloxacin combinations: a randomised trial. Lancet **380:**986–993. http://dx.doi.org/10.1016/S0140-6736(12)61080-0.
24. **Diacon AH, Pym A, Grobusch M, Patientia R, Rustomjee R, Page-Shipp L, Pistorius C, Krause R, Bogoshi M, Churchyard G, Venter A, Allen J, Palomino JC, De Marez T, van Heeswijk RP, Lounis N, Meyvisch P, Verbeeck J, Parys W, de Beule K, Andries K, Mc Neeley DF.** 2009. The diarylquinoline TMC207 for multidrug-resistant tuberculosis. N Engl J Med **360:**2397–2405. http://dx.doi.org/10.1056/NEJMoa0808427.
25. **Deknuydt F, Roquilly A, Cinotti R, Altare F, Asehnoune K.** 2013. An *in vitro* model of mycobacterial granuloma to investigate the immune response in brain-injured patients. Crit Care Med **41:**245–254. http://dx.doi.org/10.1097/CCM.0b013e3182676052.